ELSEVIER

International Journal of Mass Spectrometry 194 (2000) 41–48

International Journal of Mass Spectrometry

Ion transmission and ion/molecule separation using an electrostatic ion guide in chemistry ionization mass spectrometry

Renyi Zhang[a], Wenfang Lei[a], Liusa T. Molina[b], Mario J. Molina[b,*]

[a]*Department of Meteorology, Texas A&M University, College Station, TX 77843, USA*
[b]*Department of Earth, Atmospheric, and Planetary Sciences and Department of Chemistry, Massachusetts Institute of Technology, Cambridge, MA 02139, USA*

Received 17 November 1998; accepted 13 July 1999

Abstract

The performance of an electrostatic ion guide for use in chemical ionization mass spectrometry is evaluated. The study focuses on the use of the ion guide to extract charged particles in a rapidly expanding beam consisting of ions and neutral molecules. A theoretical analysis of this system is presented, using three-dimensional calculations of the trajectories of ions. Laboratory measurements verifying the theoretical calculations are also reported. The results illustrate the two principal advantages for this system: efficient ion transmission and ion–neutral molecule separation. A comparison between the ion guide and the commonly used electrostatic ion lenses shows that the ion guide is significantly more efficient in capturing and transporting charged particles from a diverging ion source. (Int J Mass Spectrom 194 (2000) 41–48) © 2000 Elsevier Science B.V.

Keywords: Electrostatic ion guide; Chemical ionization; Ion–molecule separation; Ion-transmission efficiency

1. Introduction

Chemical ionization mass spectrometry (CIMS) has been widely used in atmospheric chemistry research—for instance, in laboratory kinetics studies [1–3] and in atmospheric trace gas measurements [4–6]. Such applications often require extraction of ionic species from a high-pressure source (ranging from 1 Torr to 1 atm) and subsequent transmission of the charged particles into a mass analyzer operating in a low pressure regime (typically $<10^{-6}$ Torr). Hence the development of techniques for efficient ion transmission and ion/molecule separation is critical to improve the detection sensitivity in CIMS.

In a recent note, we described the design of an electrostatic ion guide for use in CIMS [7]. We placed the ion guide, consisting of an outer conductive mesh cylinder and an inner wire suspended along the central axis of the cylinder, in a low pressure chamber ($<10^{-5}$ Torr) between two charged apertures. The ion guide has been used in the past for many different applications, e.g. in orbitron ionization gauge [8,9], in analyzing nuclear particles from a remote high flux reactor [10], in time-of flight of mass spectrometry [11–16], in the presence of a magnetic field [17,18], and most recently in electrospray ionization time-of-flight mass spectrometry [19]. In those earlier studies,

* Corresponding author. E-mail: mmolina@mit.edu

PII S1387-3806(99)00161-X

the ion guide has been employed exclusively as a transport device for charged particles. The potential application of the ion guide for ion/molecule separation has not been explored.

The advantage of our design of the ion guide in the CIMS system [7] lies on its efficiency for ion transmission, its ability to separate ions from molecules, and its simplicity. In our configuration, the ion guide is positioned immediately behind a front aperture of about 0.5 mm diameter, where a diverging beam is generated due to rapid expansion of ions and molecules from about 10 Torr to less than 10^{-5} Torr. The generation of an expanding beam enables the efficient separation of ions from neutral molecules. Charged particles are captured and transported by the ion guide to the second aperture leading to the mass analyzer, whereas neutral molecules are separated and removed by a differentially pumped system as they move through the mesh of the outer cylinder of the ion guide. The charged particles passing through the front aperture are subjected to complex electrostatic and fluid dynamic forces (due to expansion); the radial and angular distributions of ion intensity in this region have not been solved analytically [20].

In this article, we analyze the use of an ion guide for capturing and transporting charged particles in a rapidly expanding beam consisting of ions and neutral molecules. Both ion transmission and ion/molecule separation were investigated by means of theoretical calculations and experimental verifications. We also present a comparison of the performances of the ion guide and electrostatic ion lenses used in an expanding ion source.

2. Results and discussion

2.1. Separation of ions and neutral molecules

In general, a gas flow passing through a circular aperture separating two regions with different pressures can either be effusive or a free jet expansion [21,22]. An effusive flow, which occurs when the molecular mean free path is much larger than the diameter of the aperture, is a good approximation to our experimental conditions. According to kinetic theory, the total gas current, N, issuing through a circular aperture from a source where the gas number density is n_s, is given by

$$N = n_s \nu \pi D^2/16 \tag{1}$$

where $\nu = (8kT/\pi m)^{1/2}$ is the molecular thermal velocity, k the Bolzmann constant, T the temperature, m the molecular weight, and D the aperture diameter. The molecular flux density, J, is related to the angle, θ, measured between the direction normal to the plane of the aperture and the direction of observation, by

$$J = N \cos\theta/(\pi L^2) = n_s \nu D^2 \cos\theta/(16L^2) \tag{2}$$

where L is the distance between the source and the point of detection of the molecules. With conservation of molecules, i.e. $J = n\nu$, the number density of beam molecules at the observation direction is expressed by

$$n = n_s D^2 \cos\theta/(16L^2) \tag{3}$$

Thus, the maximum concentration occurs on axis, defined by $\theta = 0$ or $\cos\theta = 1$. Eq. (3) indicates that the molecular density decreases rapidly as the observation point moves away from the source. Under our laboratory conditions [7], a decrease of more than two orders of magnitude in the density of beam molecules is expected at the exit end of the ion guide. In addition, the generation of an expanding beam after the front aperture allows for efficient separation of ions and neutral molecules. Charged particles are captured and transported by the ion guide, whereas neutral molecules are efficiently removed by a diffusion pump through the ion guide cylinder, which is made of a mesh screen.

Table 1 lists the pressures monitored at various stages in our differentially pumped system. Using a 0.5-mm-diameter exit aperture, a nearly 50-fold pressure rise in the ion guide chamber resulted in only a 2-fold pressure increase in the chamber housing the mass analyzer, largely due to a reduced beam intensity and resultant higher pumping conductance. Hence, our system permits efficient separation and removal of neutral molecules.

Table 1
Pressure measurements at various stages in the CIMS system

P(FT)[a] (Torr)	P(IG)[b] (Torr)	P(MS)[c] (Torr)
10.8	2.1×10^{-5}	8.2×10^{-8}
8.9	1.6×10^{-5}	7.3×10^{-8}
6.9	1.1×10^{-5}	6.4×10^{-8}
4.7	6.5×10^{-6}	5.1×10^{-8}
2.9	3.5×10^{-6}	4.6×10^{-8}
0.9	1.2×10^{-6}	4.1×10^{-8}
0.2	6.3×10^{-7}	3.5×10^{-8}

[a] P(FT) = pressure in the flow tube.
[b] P(IG) = pressure in the ion guide chamber.
[c] P(MS) = pressure in the mass spectrometer chamber.

2.2. Calculations of ion trajectories

Two-dimensional (2-D) ion trajectory calculations for the electrostatic ion guide have been performed by Limbach et al. [18] and recently by Bondarenko and Macfarlane [20]. We present here three-dimensional ion trajectory simulations with various parameters for the injected ions and the ion guide using SIMION 3D Version 6.0 [23]. The mean free path in our system is estimated to be on the order of 10^5 cm. Hence, collisions between ions and neutral molecules within the ion guide are neglected in our study.

Typical ion trajectories within the ion guide are illustrated in Fig. 1, assuming that all ions have a negative unity charge and 100 atomic mass units (u). The geometry of the ion guide is based on the experimental configuration that we reported previously [7]: the cylinder is 2 cm in diameter and 15 cm in length. In these calculations, another electrode, with a 6-mm-diameter central aperture, is located at the exit end of the guide to collimate the charged particles. In Fig. 1(a), an ion trajectory is presented in the x–y plane and in three dimensions. The central wire is held at 0 V and the outer cylinder is held at −40 V. The ion is initially injected 2 mm away from the z axis with an azimuth angle (measured between the z axis and the projection of the direction vector on the x–z plane) of 10°. The initial kinetic energy of the ion is 4 eV. Fig. 1(a) shows that the ion attains ~9 spiral orbits before emerging from the other end of the guide. The minimum orbital radius around the central

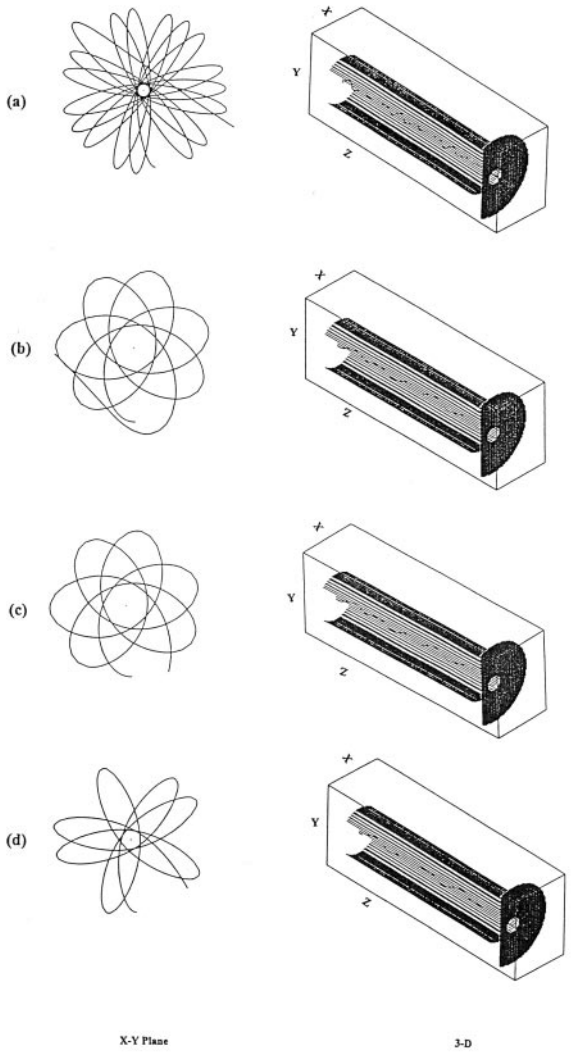

Fig. 1. Theoretical ion trajectories in an ion guide computed for an ion of unit negative charge and 100 u, viewed in the xy plane and in three dimensions (which are scaled differently). The ion enters the guide 2 mm off the z axis and is transmitted through the guide into an aperture of 6 mm diameter. (a) The initial kinetic energy of the ion is 4 eV, with an azimuth angle of 10°. Voltages are −40 V on the cylinder and 20 V on the back aperture, whereas the central wire is held at ground. (b) Same as (a) except for an initial kinetic energy of 40 eV for the ion. (c) Same as (c) except for voltages of −80 and −40 V on the cylinder and the central wire, respectively. (d) Same as (c) except for an azimuth angle of 5°.

wire is ~0.15 mm, larger than the radius of the wire (0.035 mm). The voltage applied to the exit aperture plays a role only in focusing and accelerating the ions;

it has no effect on the ion trajectory inside the guide. Fig. 1(b) shows another ion trajectory with conditions similar to those in Fig. 1(a), except for an initial ion kinetic energy of 40 eV. In this case the number of spiral orbits is reduced, with a minimum orbital radius of ~0.6 mm. With the central wire at −40 V and the cylinder at −80 V, the trajectory displayed in Fig. 1(c) does not change appreciably from that in Fig. 1(b), indicating that the absolute voltages on the cylinder and on the wire are not as critical as the voltage difference between the two. The minimum orbital radius around the central wire is about 0.6 mm. For ions with initial kinetic energies between 2 and 40 eV, we have estimated an optimum voltage difference of 10–70 V to most effectively transmit ions through the exit aperture. Fig. 1(d) shows that a smaller azimuth angle leads to a reduced minimum orbital radius (~0.28 mm). Hence, in all cases illustrated in Fig. 1, the ions execute similar trajectories, except for the orbital radius about the central axis. The ion guide appears capable of transmitting ions of various initial kinetic energies, which are initially displaced from the *z* axis and have trajectories divergent from the *z* axis.

It should be noted that one advantage for using the three-dimensional (3-D) calculations is that the interaction between the ions and the central wire is best demonstrated with views on both *xy* and *yz* planes, such as those shown in Fig. 1. A 2-D ion trajectory on the *yz* plane, on the other hand, cannot be representative of that on the *xy* plane. For example, for a calculation similar to that presented in Fig. 1(a) except with the ion trajectory initiated along the central axis, the trajectory may exhibit some spiral motion on the *yz* plane, but with repeated crossings over the central wire on the *xy* plane.

As mentioned above, charged particles passing through the front aperture separating two pressure regimes are subjected to combined electrostatic and fluid dynamic effects. To simulate the behavior of ion capture and transmission by the ion guide in an expanding beam, we have performed ion trajectory calculations using ions injected into the guide at different azimuth angles and with certain initial kinetic energies. Fig. 2 shows ion trajectory calculations using a slightly different geometry for the ion guide,

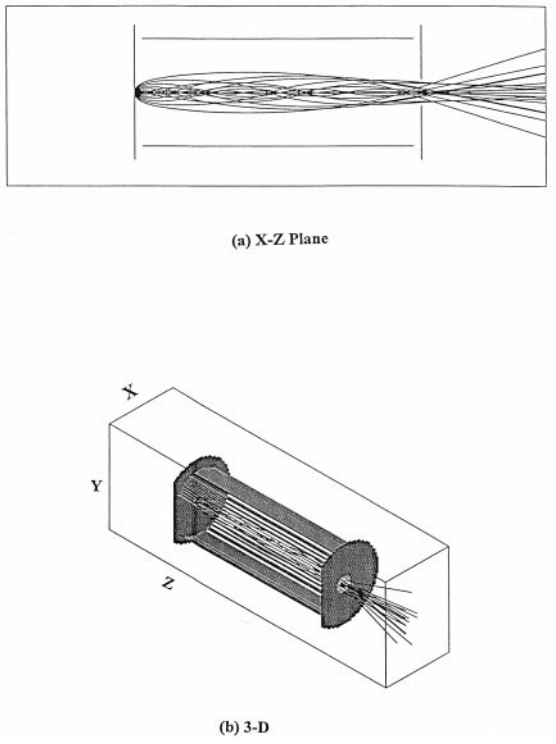

Fig. 2. Trajectories in an ion guide for a negative ion of unit charge and 100 u, viewed in the *xz* plane (a) and in the three dimensions (b). The ion enters the guide 0.01 mm off the *z* axis with an initial kinetic energy of 5 eV and with various azimuth angles with 10° increments. Voltages are −40 V on the front aperture, 10 V on the cylinder, and 0 V on the back aperture and the central wire.

based on another CIMS system that we employed recently. The ion guide is 4 cm in diameter and 10 cm in length. The diameters for the front and back apertures are 0.1 and 1 cm, respectively. The separations between the ion guide and the front and back apertures are 0.3 cm. To realistically simulate distributions of the ion density immediately after the front aperture, an ion beam—with a negative unity charge 100 u, an initial kinetic energy of 5 eV, and a 10° increment in the azimuth angle—is injected at a position 0.01 cm off the *z* axis. The voltages applied on the various electrodes are based on the optimum experimental conditions for this system, as inferred from the measured highest intensity for the reagent ions in the laboratory. The voltages are −40 V on the front aperture, 0 V on the central wire and the back

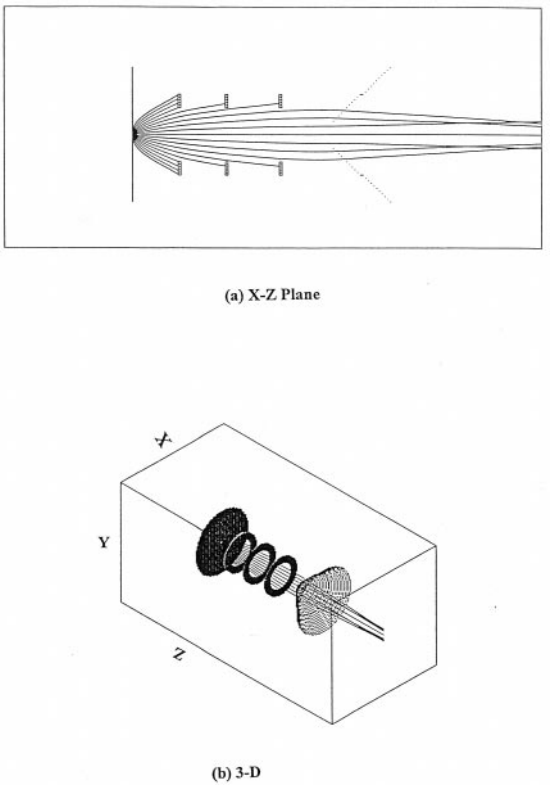

Fig. 3. Trajectories in a set of electrostatic lenses for a negative ion of unit charge and 100 u, viewed in the *xz* plane (a) and in three dimensions (b). The ion enters the center of the front aperture with an initial kinetic energy of 5 eV and with various azimuth angles with 10° increments. Voltages are −125 V on the front aperture, 150 V on the skimmer, and −100, −50, and 0 V on the first, second, and third lens, respectively.

aperture, and −10 V on the cylinder, respectively. Fig. 2 shows that a 10 V potential difference between the cylinder and the central wire for the ion guide is sufficient to transport ions at all the given azimuth angles. As discussed below, the use of various azimuth angles for ions with an initial kinetic energy of a few electron volts enables simulations of ion density distributions from a diverging ion source. The results depicted in Fig. 2, in conjunction with Eq. (3), can be applied to determine the ion transmission efficiency for the ion guide.

For comparison, we have also performed calculations of ion trajectories relevant to the use of conventional electrostatic lenses in CIMS (Fig. 3). The

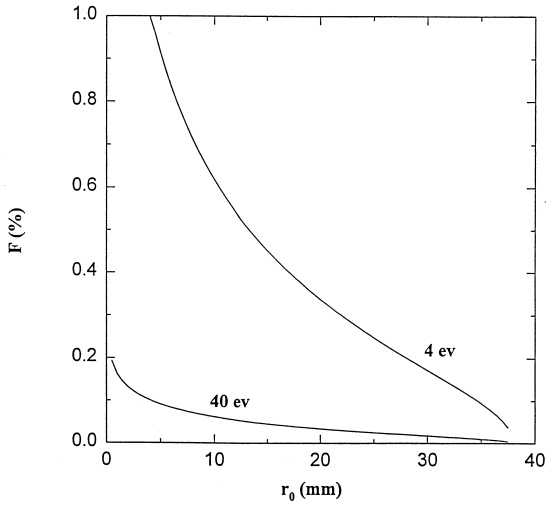

Fig. 4. Fraction of ions transmitted through the ion guide vs. initial injection radius r_0 relative to the central axis for the case of a point ion source at r_0. Calculations were made using $R = 38$ mm, $s = 0.035$, $V = 50$ V, and $q = 1$.

configuration of the ion optical system is similar to that used previously in our laboratory [1]. Briefly, negative ions are extracted through an aperture biased negatively, followed by a set of three electrostatic lenses, and further collimated by a skimmer biased positively. The voltages applied on the various electrodes are based on the optimal values obtained experimentally in the laboratory. Fig. 4 shows that, except for ions with a smaller azimuth angle (<12°), the majority of ions are unable to reach the small orifice on the skimmer. Similar calculations have been performed using various combinations of voltages applied on the lenses. In all cases, the electrostatic lenses exhibit lower ion transmission efficiency. This is largely a consequence of ion divergence resulting from the expansion after the front aperture, which is effectively simulated by assuming an initial kinetic energy of a few electron volts and an injection angle for the charged particles. On the other hand, our calculations indicate that the efficiency of the lens system increases as the kinetic energy of the charged particles decreases to values close to those characteristic of the thermal velocity of the particles. We conclude that the ion guide is more efficient than the

conventional electrostatic lens in capturing and transporting ions from a diverging ion source.

2.3. Ion transmission efficiency

For an ion injected into a potential field between two concentric cylindrical conductors with an initial velocity and a distance to the central wire, the velocity component along the z axis transports the particle down the guide and remains unchanged. The perpendicular velocity component leads to a spiral motion around the wire.

The initial kinetic energy (E) and position coordinates of the ion, along with the characteristics of the guide, determine the conditions under which an ion can achieve a bound orbit. For every particle that enters into a bound orbit, there is an apogee and perigee which are periodically achieved (Fig. 1). For a given initial injection radius (r_0), the largest injection angle relative to the central axis will be determined by the maximum allowable apogee radius, which is equal to the cylinder radius R. Assuming a point source at r_0, at which ions are emitted uniformly in a 4π geometry, the fraction of ions transmitted through the ion guide is given by a simple relation [11],

$$F(r_0) = (3qV/E)[\ln(r_0/R)/\ln(s/R)](1 - r_0^2/R^2)^{-2} \quad (4)$$

where q is the ion charge, s the radius of the wire, R the radius of the outer diameter, and V the potential difference between the two conductors. Fig. 4 shows the calculated transmission efficiency using our experimental conditions and at two different initial kinetic energies. It is evident from Fig. 4 that the transmission efficiency decreases with increasing initial kinetic energy and as the initial injection radius approaches that of the outer cylinder. For an initial ion kinetic energy of 4 eV, a transmission efficiency of unity is attained at an injection radius of less than 4 mm from the central wire.

Similarly, if the perigee of the ion orbit has a minimum radius less than that of the central wire, an ion collides with the central wire on the first orbit and is lost. To account for this effect a correction factor

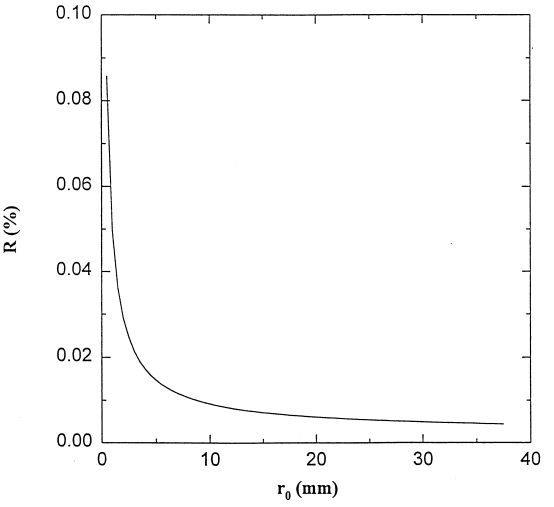

Fig. 5. Ratio of the fraction of ions achieving a bound orbit, but lost to the central wire, to the total number of ions achieving bound orbit for the case of a point ion source at r_0. Calculations were made using $R = 38$ mm and $s = 0.035$.

can be defined in terms of the ratio of the fraction of particles that achieve a bound orbit, but hit the central wire, to the total fraction of ions achieving the bound orbit. For a point ion source at an injection radius r_0, this ratio $R(r_0)$ can be expressed as [11]

$$R(r_0) = [2s/(\pi r_0)][(\eta_2/\eta_1)^{1/2} + (\eta_3/\eta_1)] \cdot \ln[(\eta_1^{1/2} + \eta_2^{1/2})/\eta_3^{1/2}][1 - (r_0^2/R^2)]^{1/2} \quad (5)$$

where $\eta_1 = \ln(R/r_0)$, $\eta_2 = \ln(R/s)$, and $\eta_3 = \ln(r_0/s)$. Fig. 5 shows that the number of ions lost on the central wire decreases as the injection radius r_0 increases. Under conditions similar to those in the present experiments, the loss of ions due to collision with the central wire would be small [$R(r_0) < 0.1$], if the ion enters the guide at an initial radius of more than 0.5 mm from the central wire, as depicted in Fig. 5. Note that this fractional loss of ions by collision with the central wire is independent of the ion initial kinetic energy, charge, and the potential difference in the guide. The overall transmission efficiency can be obtained by combining $F(r_0)$ and $R(r_0)$. For example, ions originating from a point source at a distance of 0.5 mm to the central wire with an initial kinetic energy of 4 eV would have an overall transmission efficiency of about 90%, according to Figs. 4 and 5.

Table 2
Current measurements on various conductors in the CIMS system[a]

Conductor	Current (nA)	Conditions[b]
Front aperture	-1.6×10^3	
Outer cylinder	−540	V_r and V_c grounded
Central wire	−7	$V_o = -52$ V, V_r grounded
	−0.5	V_o and V_r grounded
Rear aperture	−360	$V_o = -52$ V, V_c grounded
	−12	V_o and V_c grounded

[a] Current measurements conducted for conditions pertinent to Fig. 1, using SF_6^- ions.
[b] V_o, V_c, and V_r are voltages applied to the outer cylinder, central wire, and rear aperture, respectively. Except for the first entry, the front aperture is held at −60 V.

We have performed laboratory measurements to experimentally evaluate the ion transmission efficiency through the ion guide in our CIMS system. Ion current density and distribution in our CIMS system were measured by a picoammeter on the various electrodes, including the ion currents on the entrance and exit aperture plates, the outer cylinder, and the central wire. The picoammeter (Keithley Model 485) has an accuracy of 0.1 nA on the lowest range (2 nA scale). SF_6^- ions, formed by electron attachment through a negative corona discharge, were used for the current measurements. To account for the total ion current intercepted by the outer cylinder, the mesh cylinder was covered by a thin aluminum sheet of similar dimensions to prevent ions leaking through the mesh grid. Ions transmitted through the guide produced a current on the exit aperture plate, which had a small aperture of 10 μm in diameter to minimize the number of ions passing through the orifice.

Results of the current measurements are summarized in Table 2. It is clear from these results that the ion current transmitted through the guide increased markedly when appropriate voltages were applied. With all the electrodes (except the entrance aperture) held at ground, the sum of the currents monitored on the outer cylinder, the central wire, and the exit aperture plate—which together encompassed more than 99% of all possible surface area of ion exit path—should reflect the total ion current entering the guide. An ion transmission efficiency can then be estimated from the ratio of the ion current at the exit end of the guide to the total current. By using values listed in Table 2, an ion transmission efficiency of 0.65 was inferred, with an estimated uncertainty of about 25%. The fraction of ion loss due to collisions with the central wire, on the other hand, was negligible, less than 2%. This implies that the majority of ions were injected into the guide off z axis and had initial velocities divergent from the z axis, since ions emitted either on axis or with a zero azimuth angle would otherwise collide with the central wire.

In separate experiments, we measured a slightly higher ion transmission efficiency of 82% for the conditions pertinent to Fig. 2. When the ion guide was removed from the system, we found no observable signal ($<$0.4 nA) on the exit aperture plate. This may arise because of a nearly complete loss of ions when traveling through a relatively long distance between the two apertures. When a set of three equally spaced electrostatic lenses was mounted between the front aperture and an exit skimmer, as shown in Fig. 3, we measured a relatively weak ion current on the skimmer, about −72 nA. Assuming the same ion total current through the front aperture (i.e. with the same total aperture diameter) as that given in Table 2, this leads to a transmission efficiency of about 13%. Hence, the electrostatic lenses have a rather low efficiency of ion transmission in our CIMS system, compared to that of the ion guide. Although we did not further optimize the design for the electrostatic lenses, it appears unlikely that any other simple lens arrangement will have a higher ion transmission than that of the ion guide.

For an ion beam formed as a result of expansion after the front aperture, the ion density distribution should also comply with the cosine law of emission,

as given by Eq. (3), except that the velocity term should be related to the appropriate kinetic energy of the ions. The ion transmission efficiency is then simply the integral of Eq. (3) (i.e. cosine integration with respect to the azimuth angle) divided by the total ion density passing through the front aperture. The results shown in Figs. 2 and 3 lead to transmission efficiencies of ~100% and 20% for the ion guide and for the electrostatic lenses, respectively. These values are consistent with those measured experimentally, considering the uncertainties of our measurements and the assumptions in the theoretical calculations. Hence the ion trajectory simulations presented in Figs. 2 and 3 appear to reflect reasonably well the features of ion divergence, capture, and transmission by the ion guide and the electrostatic lenses in our CIMS systems.

3. Conclusions

In this article we have presented an analysis of the electrostatic ion guide for use in CIMS. Both theoretical calculations and laboratory experiments reveal high ion transmission efficiency and efficient ion/molecule separation. The ion guide developed has been successfully used to detect both positive and negative ions formed from chemical ionization sources: the difference in detecting the two types of ions involves only changing polarity for all the electrodes. Since the ion trajectories are only sensitive to the potential difference between the cylinder and the central wire, for simplicity the central wire can be held at ground. The ability to transport ions over a reasonably long distance offers a way to enhance the conductance (at a given pumping speed) or, alternatively, to increase the pumping speed with a higher-capacity pump. In either case, the detection sensitivity can be improved by enlarging the sizes of both the front and the rear apertures. Hence, the ion guide, which is easy to construct, provides an efficient way to improve the sensitivity in CIMS.

Acknowledgements

This work was partially supported by grants from NASA Upper Atmospheric Research Program and the U.S. Air Force Office of Scientific Research to MIT. One of the authors (W.L.) was supported by a graduate fellowship from the Robert A. Welch Foundation.

References

[1] M.J. Molina, L.T. Molina, R. Zhang, R.F. Meads, D.D. Spencer, Geophys. Res. Lett. 24 (1997) 1619.
[2] J.V. Seeley, R.F. Meads, M.J. Elrod, M.J. Molina, J. Phys. Chem. 100 (1996) 4026.
[3] R. Zhang, M.T. Leu, L.F. Keyser, J. Phys. Chem. 101 (1997) 3324.
[4] F.L. Eisele, Int. J. Mass. Spectrom. Ion Processes, 54 (1983) 119.
[5] F. Arnold, A.A. Viggiano, in Middle Atmosphere Programme, R.A. Goldberg (Ed.), Handbook for MAP, International Council od Scientific Unions, Urbana, IL, 1986, Vol. 19, pp. 102–137.
[6] O. Mohler, Th. Reiner, F. Arnold, Rev. Sci. Instrum. 64 (1993) 1199.
[7] R. Zhang, L.T. Molina, M.J. Molina, Rev. Sci. Instrum. 69 (1998) 4002.
[8] S. Kofel, M.A. Anderson, and R.E. Smalley, Rev. Sci. Instrum. 61 (1990) 3686.
[9] R.G. Herb, T. Pauly, K.J. Fisher, Bull. Am. Phys. Soc. 8 (1963) 336.
[10] W.G. Mourad, T. Pauly, R.G. Herb, Rev. Sci. Instrum. 102 (1964) 661.
[11] N.S. Oakey, R.D. Macfarlane, Nucl. Instrum. Methods 102 (1967) 220.
[12] J.C. Abbe, S. Amiel, R.D. Macfarlane, Nucl. Instrum. Methods 102 (1972) 73.
[13] R. Igersheim, J.C. Abbe, J.M. Paulus, S. Amiel, Nucl. Instrum. Methods 109 (1973) 301.
[14] R.D. Macfarlane, D.F. Torgerson, Int. J. Mass Spectrom. Ion Processes 21 (1976) 81.
[15] A. Kenigsberg, J. Leon, N.H. Shafrir, Nucl. Instrum. Methods 148 (1978) 605.
[16] P.W. Geno, R.D. Macfarlane, Int. J. Mass Spectrom. Ion Processes 74 (1986) 43.
[17] C.E. Johnson, J. Appl. Phys. 55 (1984) 3027.
[18] P.A. Limbach, A.G. Marshall, M. Wang, Int. J. Mass Spectrom. Ion Processes 125 (1993) 135.
[19] O. Klemperer, Electron Optics (Cambridge University Press, New York, 1971).
[20] P.V. Bondarenko, R.D. Macfarlane, Int. J. Mass Spectrom. Ion Processes 160 (1997) 241.
[21] J.A. Laurmann, Rarefied Gas Dynamics, Academic, New York, 1963, Vol. I.
[22] J. de Leeuw, Rarefied Gas Dynamics, Academic, New York, 1966, Vol. II.
[23] D.A. Dahl, SIMION 3D, Version 6.0, Idaho National Engineering Laboratory, 1995.